International Journal for Modern Trends in Science and Technology
Volume 12, Issue 04, pages 766-776
ISSN: 2455-3778 online
Available online at: http://www.ijmtst.com/vol12issue04.html
DOI: https://doi.org/10.5281/zenodo.19567157

Solar PV System with MPPT (Perturb & Observe) Using Simulink

P. Nagarjuna, Ch. Harshitha, Ch. Satya Sravani, G. Padma, G. Kalyani

Department of Electrical and Electronics Engineering, Vasireddy Venkatadri Institute of Technology, Pedakakani, Namburu, Guntur, India.

To Cite this Article
P. Nagarjuna, Ch. Harshitha, Ch. Satya Sravani, G. Padma & G. Kalyani (2026). Solar PV System with MPPT (Perturb & Observe) Using Simulink. International Journal for Modern Trends in Science and Technology, 12(04), 766-776. https://doi.org/10.5281/zenodo.19567157

Article Info
Received: 16 March 2026; Revised: 06 April 2026; Accepted: 10 April 2026.

KEYWORDS

Solar Photovoltaic (PV), Hybrid Energy System, Battery Energy Storage, Supercapacitor, Bidirectional Buck–Boost Converter, EV Charging, Renewable Energy Integration, Maximum Power Point Tracking (MPPT), Perturb and Observe (P&O), Energy Management, Electric Vehicle (EV).

ABSTRACT

This paper presents the design and analysis of a multi-source DC-link integrated energy system incorporating a solar photovoltaic (PV) source, battery storage, supercapacitor, and electric vehicle (EV) load for improved energy management and system reliability. The PV system is interfaced through a DC–DC boost converter controlled by a Perturb and Observe (P&O) maximum power point tracking algorithm to ensure optimal power extraction under varying irradiance conditions. A bidirectional buck–boost converter is employed for the battery to enable controlled charging and discharging operations, while a supercapacitor is integrated through a similar converter to handle transient power fluctuations and reduce dynamic stress on the battery, thereby enhancing its lifespan. The system supports multiple loads, including DC loads, AC loads, and EV battery charging. The EV battery is interfaced using a dedicated buck–boost converter to ensure regulated power flow. An inverter with dq-based voltage and current control is utilized for supplying AC loads, ensuring improved power quality and stable operation. All energy sources and loads are interconnected through a regulated DC-link voltage, which serves as the central energy management node. The proposed configuration enables efficient power sharing, improved dynamic response, and enhanced system stability under varying operating conditions. Simulation results validate the effectiveness of the system in achieving reliable performance, reduced battery stress, and optimal utilization of renewable energy, making it suitable for modern hybrid energy and EV applications.

1. INTRODUCTION

The rapid increase in global energy demand, along with growing environmental concerns and the depletion of conventional fossil fuel resources, has significantly accelerated the transition toward renewable energy-based power systems. Among the various

renewable energy sources, solar photovoltaic (PV) systems have emerged as one of the most promising solutions due to their abundance, modularity, scalability, and decreasing installation costs [1]–[3]. Despite these advantages, PV systems are inherently intermittent and highly dependent on environmental conditions such as solar irradiance and temperature, which leads to fluctuations in output power and challenges in maintaining a stable energy supply [4], [5]. To overcome the limitations of PV systems, energy storage technologies have been widely integrated into renewable energy systems to enhance reliability and ensure continuous power delivery. Battery energy storage systems (BESS) are commonly used due to their high energy density and capability to store energy for extended periods [6], [7]. However, batteries are prone to degradation when subjected to high-frequency charge–discharge cycles, peak current stresses, and deep discharges, which significantly reduce their lifespan and efficiency [8], [9]. On the other hand, supercapacitors offer high power density, rapid response, and long cycle life, making them suitable for handling transient power demands and smoothing short-term fluctuations [10], [11]. Therefore, combining batteries and supercapacitors into a hybrid energy storage system (HESS) provides a complementary solution that enhances overall system performance, efficiency, and durability [12], [13]. In recent years, the increasing adoption of electric vehicles (EVs) has further intensified the need for efficient and reliable energy management systems. EVs are considered a sustainable alternative to conventional internal combustion engine vehicles, contributing to reduced greenhouse gas emissions and improved energy efficiency [14], [15]. However, the integration of EV charging infrastructure with renewable energy sources introduces challenges such as fluctuating load demand, grid instability, and the need for intelligent energy coordination [16]. Hybrid energy systems that integrate PV generation with storage devices and EV loads offer an effective approach to address these challenges by enabling efficient power utilization and reducing dependence on the conventional grid [17], [18].

Power electronic converters play a crucial role in facilitating the integration and control of multiple energy sources and storage elements within a unified energy system. DC–DC converters such as boost, buck, and bidirectional buck–boost converters are widely employed for voltage regulation, energy conversion, and controlled power flow between system components [19], [20]. In PV systems, Maximum Power Point Tracking (MPPT) techniques are essential to ensure maximum energy extraction under varying environmental conditions. Among the various MPPT techniques, the Perturb and Observe (P&O) method is widely adopted due to its simplicity and ease of implementation [21]. Additionally, bidirectional converters enable efficient charging and discharging of batteries and supercapacitors, supporting dynamic energy balancing and improving system responsiveness [22]. For AC load applications, voltage source inverters (VSIs) with advanced control techniques such as dq-axis (synchronous reference frame) control are utilized to ensure stable operation and improved power quality. These control strategies provide effective voltage regulation, reduced harmonic distortion, and enhanced dynamic performance under varying load conditions [23]. The concept of a DC-link integrated system has gained significant attention due to its flexibility and efficiency in managing multiple energy sources and loads. In such systems, a common DC bus serves as a central node for energy exchange, enabling coordinated control and efficient power sharing among PV sources, storage devices, and loads [24].

The development of multi-source hybrid energy systems integrating solar PV, battery storage, supercapacitors, and EV loads provides a comprehensive solution for modern energy challenges. In these systems, the supercapacitor handles fast transient power demands, the battery manages medium- and long-term energy storage, and the PV system acts as the primary energy source. This coordinated operation reduces stress on the battery, enhances system stability, and improves overall efficiency [25]. In this context, the present work focuses on the design and performance analysis of a multi-source DC-link integrated energy system incorporating a solar PV source, battery storage, supercapacitor, and EV load. The system employs a boost converter with P&O MPPT for optimal PV power extraction, bidirectional converters for battery and supercapacitor energy management, and a dedicated converter for EV charging. Furthermore, an inverter with dq-based control is used for AC load supply. The integration of these components through a regulated DC-link enables efficient power sharing, improved

dynamic response, and enhanced system reliability under varying operating conditions.

II. System Configuration

The proposed system configuration is a multi-source DC-link integrated energy system that combines a solar photovoltaic (PV) source, battery storage, supercapacitor, and multiple loads including DC load, AC load, and an electric vehicle (EV) charging unit. All components are interconnected through a common DC bus, which acts as the central node for power exchange and energy management. The solar PV system is connected to the DC bus through a DC–DC boost converter controlled by a Maximum Power Point Tracking (MPPT) algorithm to ensure maximum power extraction under varying irradiance conditions. The battery storage system is interfaced using a bidirectional buck–boost converter, allowing it to operate in both charging and discharging modes. It provides medium- and long-term energy support to maintain system reliability. The supercapacitor is also connected through a bidirectional converter and is mainly used to handle transient power fluctuations and sudden load variations due to its fast response and high power density, thereby reducing stress on the battery. The DC bus maintains a regulated voltage and supplies power to both DC and AC loads. The AC load is powered through a three-phase voltage source inverter (VSI) with appropriate filtering, ensuring stable operation and good power quality. Additionally, the EV charging station is connected via a dedicated DC–DC converter, enabling controlled charging of the EV battery. Overall, this configuration ensures efficient power sharing, improved dynamic response, and enhanced system stability.

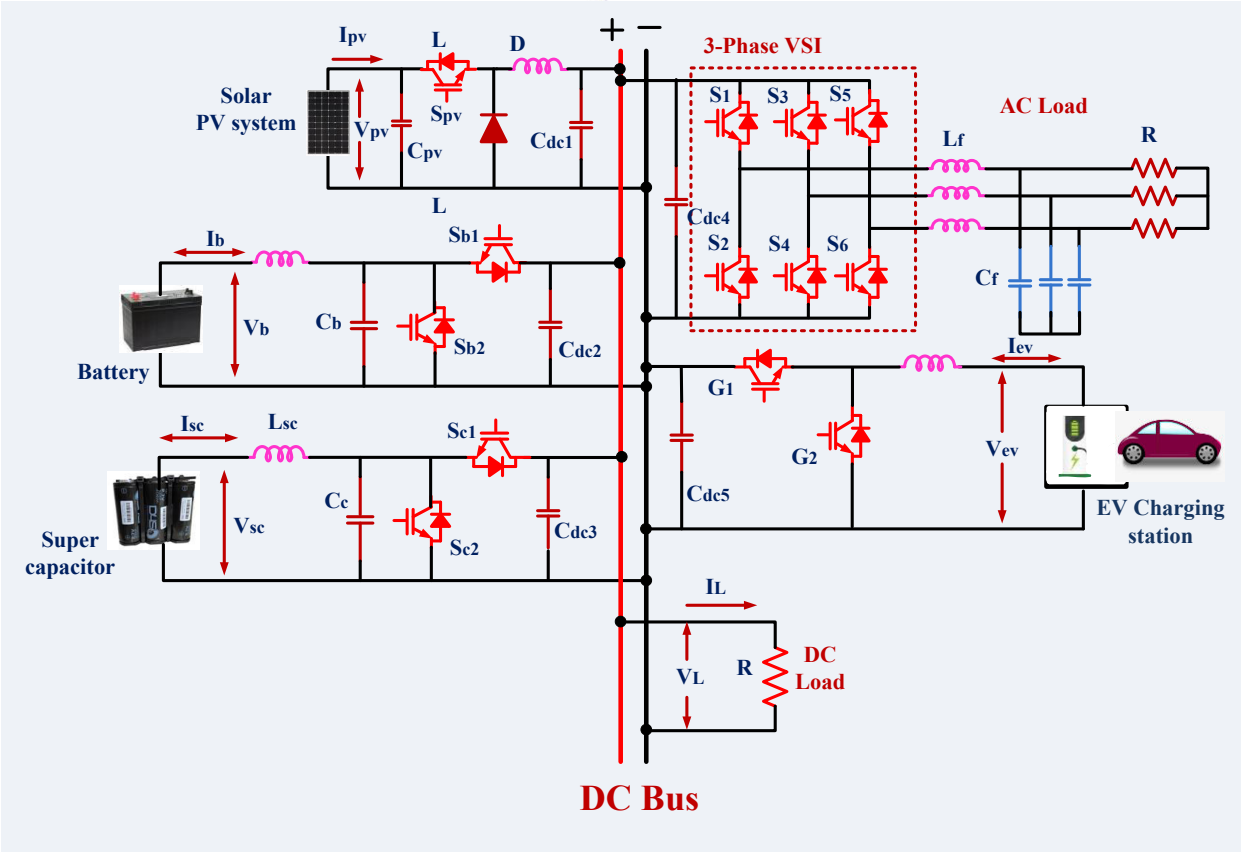

Fig.1 Overall system configuration

III. Modeling and designing of proposed system configuration

A. Modeling and Designing of Solar PV configuration

The single-diode model is a practical and widely used representation of photovoltaic (PV) cells, effectively capturing their current-voltage (I-V) characteristics while considering factors like temperature and irradiance. This model is essential for determining key performance metrics such as short-circuit current, open-circuit voltage, maximum power point, and fill factor. In practice, PV cells are connected in series and parallel to create modules, which are further combined into PV arrays. The output from these arrays is typically managed by a DC–DC boost converter that regulates

terminal voltage and enables maximum power point tracking (MPPT) by adjusting the duty cycle. This optimization enhances energy conversion efficiency, and the regulated DC output is then connected to a common DC link, which interfaces with the utility grid via a DC–AC inverter for grid-connected operations. As shown in Figure 2, PV modules based on the single-diode cell model are interconnected in series (N_s) and in parallel (N_p) to constitute a complete PV array. The equivalent output current of the PV array, considering the single-diode model, can therefore be expressed as [30]:

$$I_{pv} = N_s I_s - N_p I_o \left(\exp\left(\frac{q(V_{pv}+R_s I_{pv})}{AkTN_s}\right) - 1\right) - N_p \frac{V_{pv}+R_s I_{pv}}{N_s R_{sh}} \quad (1)$$

where Is is the light-generated current, Io is the diode reverse saturation current, R_s and R_{sh} are the series and shunt resistances, q is the electron charge, k is the Boltzmann constant, T is the cell temperature, and A is the diode ideality factor.

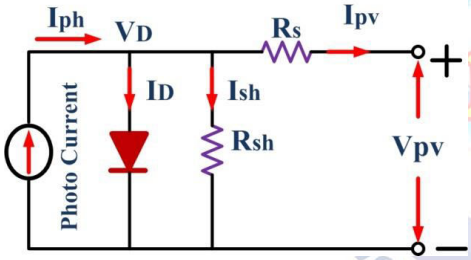

Fig.2: Equivalent circuit model of PV solar

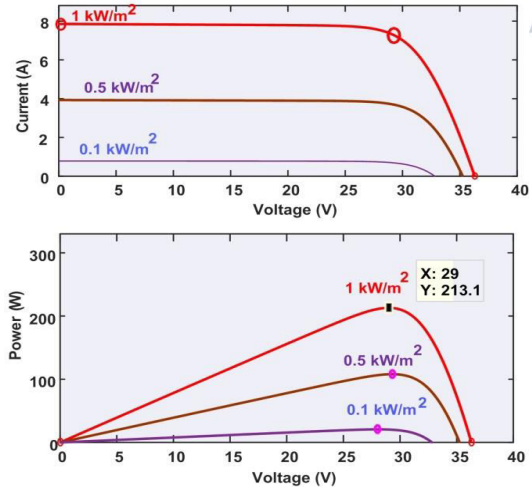

Fig 3: V–I and P–V characteristics of a single-diode PV solar cell

B. Solar PV Boost converter with P&O MPPT

A solar photovoltaic (PV) array's nonlinear current-voltage characteristics necessitate maximum power point tracking (MPPT) for optimal energy extraction. This study uses a DC–DC boost converter with the Perturb and Observe (P&O) algorithm to adjust the converter's duty cycle and regulate output voltage. While P&O is simple, it struggles with efficiency during rapid irradiance changes and can cause grid instability. As shown in Figure 4 to enhance performance, an artificial neural network (ANN)- based MPPT controller is introduced, reducing fluctuations and ensuring smooth power transfer to the grid and reliable EV battery charging.

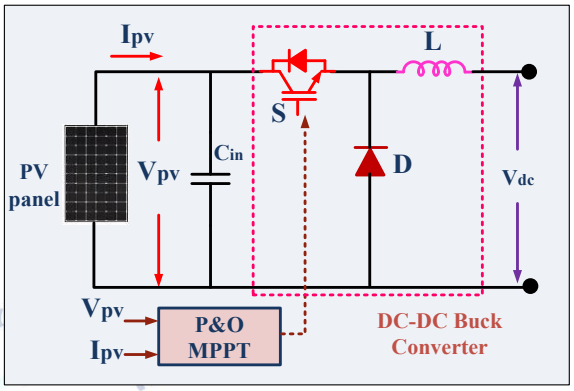

Fig.4 solar PV P&O MPPT DC-DC Buck converter

The steady-state equations of the boost converter are:

- Boost converter output voltage:

$$V_o = \frac{V_{pv}}{1-D} \quad (2)$$

- Boost converter input current:

$$I_{pv} = \frac{I_o}{1-D} \quad (3)$$

Where: V_{pv} and I_{pv} is the PV voltage and current, V_o is the DC link voltage, Io is the output current, and D is the duty cycle. The MPPT algorithm continuously updates D to regulate V_{pv} around the MPP.

b. P&O MPPT Algorithm

The Perturb and Observe (P&O) algorithm works by periodically increasing or decreasing the operating voltage and observing the effect on the power output. The key idea is:

- If ΔP>0 and ΔV>0, increase voltage.
- If ΔP>0 and ΔV<0, decrease voltage.
- If ΔP<0, reverse the last change in voltage.

The current power is calculated as:

$$P(k) = V_{pv}(k) \cdot I_{pv}(k) \quad (3)$$

And the previous power:

$$P(k-1) = V_{pv}(k-1) \cdot I_{pv}(k-1) \quad (4)$$

The MPPT controller adjusts the duty cycle D of the Buck converter accordingly.

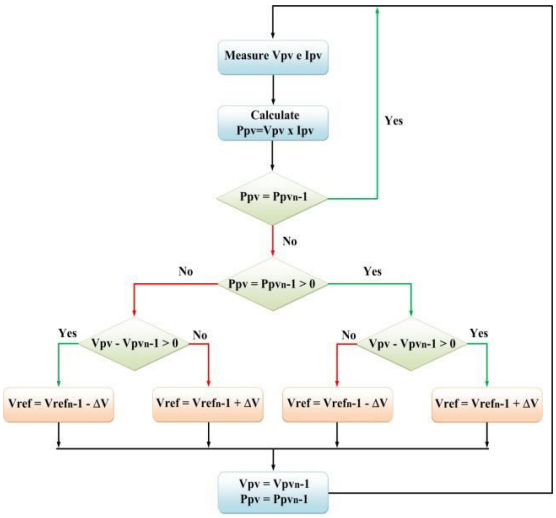

Fig .5: Flowchart of the P&O algorithm, implemented in the controller model.

IV. Modeling and Designing of a Bidirectional Buck-Boost Converter

A. Introduction and System Overview

The combined strengths of lithium-ion batteries and supercapacitors allow for hybrid energy storage devices, which take use of both technologies' high power densities and energy densities as shown in Fig.6. The DC bus and these storage parts may be effectively managed with the help of a bidirectional buck-boost converter. Power may be transported in either way, from charging storage devices to powering the load, thanks to its ability to perform both step-down (buck) and step-up (boost) operations. When the battery is being charged or discharged, or when the supercapacitor is handling high-power transients, this converter must control the voltage effectively.

B. Operating Modes

The converter operates in two primary modes:

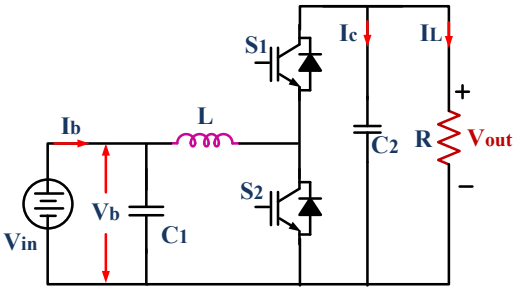

Fig.6 circuit diagram of DC-DC bidirectional buck boost converter

- **Buck Mode (Step-Down):** When the voltage on the DC bus is lower than the battery voltage (or supercapacitor voltage), the converter operates in buck mode to step down the voltage. This is typically used when discharging energy from the storage system to the bus or load.
- **Boost Mode (Step-Up):** When the voltage on the DC bus is higher than the storage voltage, the converter operates in boost mode to step up the voltage. This mode is used when charging the storage elements from the DC bus.

A single converter can operate in either mode by adjusting the duty cycle of its switching devices. In bidirectional operation, the power electronics (usually using MOSFETs or IGBTs) are arranged in an H-bridge or similar topology to allow current flow in both directions.

$$V_{out} = D \cdot V_{in} \quad (8)$$

Where: Vin is the input voltage (from the battery or DC bus), Vout is the regulated output voltage (to the load or storage device), D is the duty cycle, with 0<D<1.

3. Boost Mode (Step-Up Operation)

In boost mode, the converter increases the input voltage to a higher output voltage. The output voltage is expressed as:

$$V_{out} = \frac{V_{in}}{(1-D)} \quad (9)$$

Where: Vin is the lower voltage from the storage device or DC bus, Vout is the higher regulated voltage, D is the duty cycle, with 0<D<1.

4. Inductor and Capacitor Design

For both modes, an inductor L and output capacitor C are essential for smoothing the current and voltage ripples.

C. Inductor Design

To ensure continuous conduction mode (CCM) and limit the inductor current ripple (ΔIL), the inductor value can be estimated by:

$$L = \frac{(V_{in} - V_{out}) \cdot D}{f_s - \Delta I_L} \quad (10)$$

$$L = \frac{V_{in} \cdot D}{f_s - \Delta I_L} \quad (11)$$

Where: fs is the switching frequency, ΔIL is the desired peak-to-peak inductor current ripple.

D. Capacitor Design

The output capacitor C smooths the voltage ripple (ΔVout) at the output and is given by:

$$C = \frac{I_{out} \cdot D}{f_s - \Delta V_{out}} \quad (12)$$

Where: Iout is the load or charging current, ΔVout is the acceptable output voltage ripple.

V. Modeling and Designing of Lithium-Ion Battery and Supercapacitor.

In modern power systems, Hybrid Energy Storage Systems (HESS) integrates two or more energy storage devices to optimize power and energy performance. Lithium-ion batteries offer high energy density, making them ideal for sustained energy supply. Supercapacitors (SCs) offer high power density and rapid charge/discharge capabilities, making them ideal for handling transient loads or power fluctuations. Combining both enables better load balancing, longer battery life, and faster response times, especially in applications like EV charging, renewable integration, and microgrids.

II. A. Modeling and Designing of Lithium-Ion EV Battery

Lithium-ion (Li-ion) batteries operate on the principle of reversible intercalation and de-intercalation of lithium ions between the graphite anode and a metal oxide cathode. The overall reaction of a Li-ion cell during charge–discharge is expressed as [31]-[32]:

$$Li_xC + Li_{1-x}M_yO_z \Leftrightarrow C + L_iM_yO_z \qquad (4)$$

Where:

- Li_xC represents the lithiated graphite anode,
- $Li_{1-x}M_yO_z$ represents the partially lithiated cathode (metal oxide such as $L_iC_0O_2, L_iF_ePO_4, LiMn_2O_4$),
- M is the transition metal,
- x denotes the degree of intercalation.
- At the anode (during discharge):

$$Li_xC \longrightarrow C + xLi^+ + xe^- \qquad (5)$$

- At the anode (during discharge):

$$Li_{1-x}M_yO_z + xLi^+ \longrightarrow L_iM_yO_z \qquad (6)$$

This reaction is reversible; enabling repeated charging and discharging cycles.

Electrical Modeling

Lithium-ion batteries are commonly represented using an Equivalent Circuit Model (ECM), which simplifies the underlying electrochemical processes while accurately capturing the electrical behavior. In this model, the terminal voltage of the cell is expressed as:

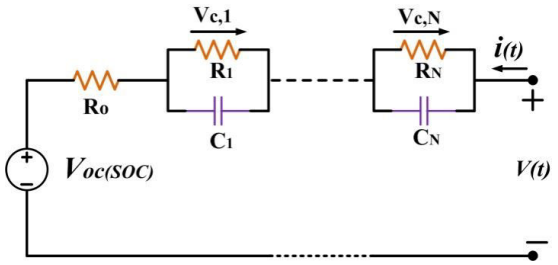

Fig.7: Equivalent circuit diagram of lithium ion EV battery

$$V(t) = V_{oc}(Soc) - I(t)R_s - V_{Rc}(t) \qquad (7)$$

The battery terminal voltage $V(t)$ is influenced by the open-circuit voltage $V_{oc}(Soc)$, internal resistance Rs, and polarization voltage $V_{Rc}(t)$. This model effectively balances accuracy and simplicity, making it ideal for grid integration, renewable energy storage, and EV charging. State of charge (SOC) measures the available charge relative to a battery's nominal capacity and changes over time based on the Coulomb counting principle.

$$SOC(t) = SOC(0) - \frac{1}{Q_{nom}}\int_0^t I(\tau)\,d\tau \qquad (8)$$

Where $SOC(0)$ is the initial SOC, Q_{nom} is the nominal battery capacity in ampere-hours (Ah), and $I(\tau)$ is the instantaneous current (positive during discharge and negative during charge). Accurate modeling of both the ECM and SOC dynamics ensures reliable performance prediction, efficient energy management, and extended lifetime of lithium-ion batteries in modern power systems.

A. Battery Converter Modeling

Lithium-ion batteries are typically modeled using electrical equivalent circuits, such as the Thevenin model or Rint (resistance-in-series) model, which account for the terminal voltage, internal resistance, and state of charge (SOC).

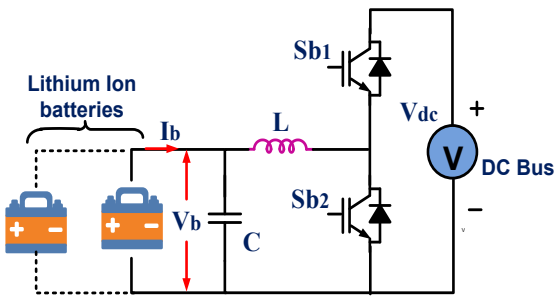

Fig.7 principle operation bidirectional dc-dc buck boost converter

a. Rint Model

The simplest model is:

$$V_{bat} = V_{OC}(SOC) \cdot I_{bat} \cdot R_{int} \quad (9)$$

Where: Vbat: terminal voltage of the battery (V), VOC (SOC): open circuit voltage as a function of state of charge, Ibat: battery current (positive for discharge, negative for charge), Rint: internal resistance of the battery (Ω)

b. State of Charge (SOC)

SOC represents the available capacity and is updated as:

$$SOC(t) = SOC(t_0) + \frac{1}{C_{out}} \int_{t_0}^{t} I_{bat}(t)\, dt \quad (10)$$

Where: SOC(t): initial SOC, Cbat: nominal capacity of the battery in Ah, Ibat(t): battery current at time t

c. Energy Stored

$$E_{bat} = C_{bat} \cdot V_{nom} \quad (11)$$

B. Supercapacitor Converter Modeling

Supercapacitors are modeled as ideal capacitors in series with a small equivalent series resistance (ESR).

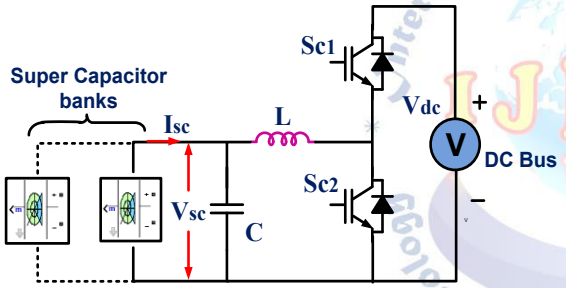

Fig.8 Super capacitor banks.

$$V_{SC}(t) = \frac{1}{C_{sc}} \int_{t_0}^{t} I_{sc}(t) + I_{SC}(t) \cdot R_{SC} \quad (12)$$

Where: VSC(t): terminal voltage of the supercapacitor, CSC: capacitance in Farads, ISC(t): current through the supercapacitor, RSC: equivalent series resistance (Ω)

a. Energy Stored

$$E_{SC} = \frac{1}{2} C_{sc} V_{sc}^2 \quad (13)$$

VI. Proposed Supervisory Power Management scheme of DC microgrid

To ensure the stable and reliable operation of a Low-Voltage DC microgrid, it is essential to regulate the DC bus voltage under all operating conditions. This guarantees smooth integration of Renewable Energy Resources (RERs) like solar PV and wind, proper load balancing, and efficient management of the Hybrid Energy Storage System (HESS), which includes a battery and a supercapacitor (SC).

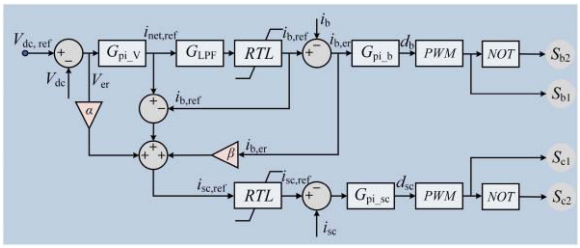

Fig. 9. Proposed modified frequency-based dual-loop control strategy of HESS.

1. DC Bus Power Balance

The total power at the DC bus must be balanced among the RERs, storage units, and loads. The overall power balance equation is given as:

$$P_{net}(t) = P_B(t) + P_{SC}(t) \quad (14)$$

Where: Pnet(t): Net power required at the DC bus, PB(t): Battery power, PSC(t): Supercapacitor power

The net power is calculated from the difference between total renewable generation and the load demand:

$$P_{net}(t) = [P_{PV}(t) + P_W(t)] - P_{load}(t) - P_{loss}(t) \quad (15)$$

Where: PPV(t): Solar PV power, PW(t): Wind power, Pload(t): Load demand, Ploss(t): Line or converter losses

2. Power and Current Dynamics at DC Bus

To maintain voltage regulation, net power can be split into average and transient components:

$$P_{net}(t) = \bar{P}_{net}(t) + \hat{P}_{net}(t) = V_{dc}(t) \cdot i_{net}(t) \quad (16)$$

This can be rewritten in terms of current as:

$$i_{net}(t) = \frac{\bar{P}_{net}(t)}{V_{dc}(t)} + \frac{\hat{P}_{net}(t)}{V_{dc}(t)} = \bar{\imath}_{avg}(t) + \hat{\imath}_{tran}(t) \quad (17)$$

Here: $\bar{i}_{avg}(t)$: Average current (handled by battery) $\hat{i}_{tran}(t)$: Transient current (handled by SC)

The net current is obtained using an outer voltage loop PI controller:

$$i_{net}(t) = \left(K_{pv} + \frac{K_{iv}}{s}\right) + \left(V_{dc,ref} - V_{dc}\right) \quad (18)$$

3. Current Splitting Using Low-Pass Filter

To separate the control actions for the battery and SC, the net current is processed through a Low-Pass Filter (LPF):

- Battery current (low-frequency component):

$$\bar{\imath}_{net}(s) = i_{net}(s) \cdot G_{LPF}(s) = i_{b,ref}(s) \quad (19)$$

- SC current (high-frequency + compensation):

$$i_{SC,ref}(s) = i_{net}(s) \cdot \left(1 - G_{LPF}(s)\right) + \alpha\left(V_{dc,ref} - V_{dc}\right) + \beta(i_{b,ref} - i_b) \quad (20)$$

Where:

- $G_{LPF} = \frac{2\pi f_\omega}{s + 2\pi f_\omega}$ is the LPF transfer function
- fco=5Hz: Experimentally selected cutoff frequency
- α, β: Feed-forward gains

- $\beta = \frac{V_b}{V_{sc}}$ Gain to improve SC response due to battery delay

4. Duty Ratio Generation for HESS Control

The reference currents $i_{sc,ref}$ and $i_{b,ref}$ are compared with actual current values to generate control signals via PI controllers:

- Battery duty ratio:

$$d_b = \left(K_{p,B} + \frac{K_{i,B}}{s}\right) + \left(i_{b,ref} - i_b\right) \quad (21)$$

- Supercapacitor duty ratio:

$$d_{sc} = \left(K_{p,sc} + \frac{K_{i,sc}}{s}\right) + \left(i_{sc,ref} - i_{sc}\right) \quad (22)$$

These duty cycles are fed to the Bidirectional Buck-Boost Converters that regulate charging/discharging operations of the HESS.

VII. Inverter Voltage and Current Controller Working and Operation

In order to power the AC load, the inverter transforms the DC power that is already present in the hybrid energy system into regulated AC power. Stable voltage, rapid dynamic response, and enhanced power quality are all achieved via the use of a dq reference frame management method. Under steady-state circumstances, the three-phase AC variables are converted into DC signals by transforming them into a rotating reference frame. Both the controller's architecture and its regulating performance are enhanced by this. A voltage control loop on the outside and a current control loop on the inside make up the typical inverter control architecture. The inverter current is made to follow the reference values by the inner loop, which controls the load-side AC voltage and creates the reference currents. Using a reference angle θ, the dq transformation is brought into synchronization with the output voltage vector. The first step is to use the Clarke transformation to convert the three-phase output voltages va, vb, and vc into the stationary frame components vα and vβ.

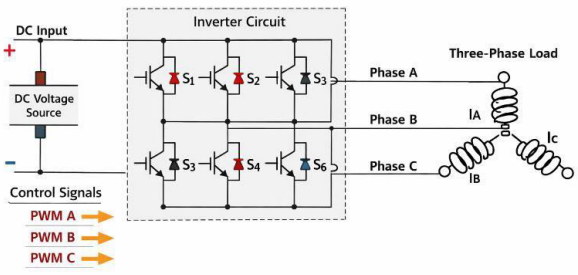

Fig.10 DC-AC inverter configuration

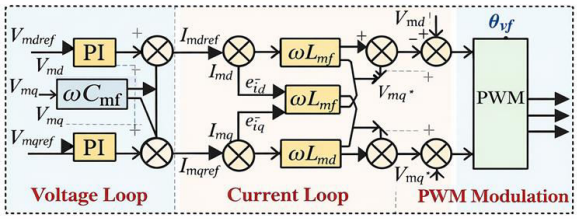

Fig.11 DC-AC inverter control strategy

$$v_\alpha = \frac{2}{3}\left(v_a - \frac{1}{2}v_b - \frac{1}{2}v_c\right) \quad (23)$$

$$v_\beta = \frac{2}{3}\left(\frac{\sqrt{3}}{2}v_b - \frac{\sqrt{3}}{2}v_c\right) \quad (24)$$

These stationary frame components are then transformed into synchronous rotating frame components vd and vq using the Park transformation:

$$v_d = v_\alpha \cos\theta + v_\beta \sin\theta \quad (25)$$

$$v_q = -v_\alpha \sin\theta + v_\beta \cos\theta \quad (26)$$

Similarly, the inverter output currents are transformed from abc to dq coordinates as id and iq. In the synchronous reference frame, the d-axis component is usually associated with active power control, while the qqq-axis component is associated with reactive power control.

For an inverter connected to an AC load through an output filter inductance Lf and resistance Rf, the dynamic equations in the dq frame are given by:

$$L_f \frac{di_d}{dt} = v_{id} - v_{od} - R_f i_d + \omega L_f i_q \quad (27)$$

$$L_f \frac{di_q}{dt} = v_{iq} - v_{oq} - R_f i_q - \omega L_f i_d \quad (28)$$

where vid and viq are the inverter control voltages in dq frame, vod and voq are the output voltages across the load or filter capacitor, ω is the angular frequency, and id , iq are the dq currents. The outer voltage controller compares the reference output voltages vd∗ and vq∗ with the measured voltages vd and vq. The corresponding voltage errors are:

$$e_{vd} = v_d^* - v_d \quad (29)$$

$$e_{vq} = v_q^* - v_q \quad (30)$$

These errors are processed through PI controllers to generate the reference currents:

$$i_d^* = K_{pv}(e_{vd}) + K_{iv}\int e_{vd}\,dt \quad (31)$$

$$i_q^* = K_{pv}(e_{vq}) + K_{iv}\int e_{vq}\,dt \quad (32)$$

where Kpv and Kiv are the proportional and integral gains of the voltage controller.

The generated reference currents are then compared with the measured dq currents to produce current errors:

$$e_{id} = i_d^* - i_d \tag{33}$$

$$e_{iq} = i_q^* - i_q \tag{34}$$

These current errors are passed through the inner current PI controllers to generate the inverter reference voltages. Including decoupling terms, the control laws are written as:

$$v_{id}^* = K_{pi}(e_{id}) + K_{ii}\int e_{id}\,dt - \omega L_f i_q + v_{od} \tag{35}$$

$$v_{iq}^* = K_{pi}(e_{iq}) + K_{ii}\int e_{iq}\,dt + \omega L_f i_d + v_{oq} \tag{36}$$

where Kpi and Kii are the proportional and integral gains of the current controller. The terms ωLfiq and ωLfid are decoupling terms that compensate the coupling between the d and q axes and improve dynamic response.

The reference voltages vid∗ and viq∗ are then converted back into αβ and abc quantities using inverse Park and inverse Clarke transformations. These three-phase reference signals are supplied to the PWM generator to produce switching pulses for the inverter switches.

The inverse Park transformation is given by:

$$v_\alpha^* = v_d^*\cos\theta - v_q^*\sin\theta \tag{37}$$

$$v_\beta^* = v_d^*\sin\theta + v_q^*\cos\theta \tag{38}$$

Then the inverse Clarke transformation gives:

$$v_a^* = v_\alpha^* \tag{39}$$

$$v_b^* = -\frac{1}{2}v_\alpha^* + \frac{\sqrt{3}}{2}v_\beta^* \tag{40}$$

$$v_c^* = -\frac{1}{2}v_\alpha^* - \frac{\sqrt{3}}{2}v_\beta^* \tag{41}$$

The inverter switches are controlled by these reference phase voltages in sinusoidal PWM or space vector PWM. The operating output voltage often drifts away from its reference as a result of variations in the AC load. This divergence is detected by the outer voltage loop, which then adjusts the reference current appropriately. Once the new reference is set, the inverter current is quickly forced to follow by the inner current loop. This allows the inverter to keep the AC voltage and current steady regardless of the load circumstances. Quick transient response, less steady-state error, and better harmonic performance are all benefits of dq control. Additionally, it allows for active and reactive power to be controlled independently, which is particularly helpful in hybrid energy systems that provide dynamic AC loads. This inverter is ideal for renewable energy systems that include AC loads because the dq-based voltage and current controller guarantees dependable operation via precise voltage regulation, efficient current tracking, and enhanced power quality.

VIII. Simulation Results and Discussion

The proposed PV-integrated DC microgrid, which includes a composite energy storage system (CESS) and a three-phase VSI, is tested under different operating situations to determine its performance. These findings show how currents, power sharing, and regulating the DC bus voltage behave dynamically. The source and storage currents, comprising PV current (Ipv), load current (IL), battery current (Ib), and supercapacitor current (Isc), are shown in Fig. 13 (a). At first, when the currents through the batteries and supercapacitors are low, the PV system provides most of the load requirement. The supercapacitor swiftly reacts to abrupt changes in load (at around 0.3 s and 0.5 s) by providing transient current support, as seen by the dramatic fluctuations in Isc. The steady-state power need is met by the battery current, which fluctuates more subtly. This demonstrates how the supercapacitor manages variations at high frequencies and how the battery supplies power at low frequencies; this allows for efficient power sharing and reduces strain on the battery. The power distribution among various components is shown in Fig. 13 (b). This includes the power from PV, DC load, batteries, supercapacitors, and AC load. It is clear that the load demand is dynamic and that PV power is conditional on operational circumstances. The battery and supercapacitor work together to make up for the shortfall in PV power during a rapid spike in demand (around half a second). Under transient situations, the supercapacitor provides brief bursts of power, while the battery helps with steady power supply. Similarly, the storage system absorbs extra PV power during periods of decreased load demand. This proves that the suggested composite energy storage technology can successfully keep power balanced and guarantee that the system runs smoothly. Voltage profile

(Vdc) of the DC bus is shown in Fig. 13 (c). The DC bus voltage is tightly controlled around its reference value, which is roughly 400 V, even when the load and generation vary. Due to the coordinated management of the converters and energy storage units, the system swiftly stabilizes after experiencing minor voltage dips and overshoots during transient events, especially around 0.5 s. The suggested control technique successfully maintains system stability, as seen by the rapid recovery of DC bus voltage. All things considered, the results prove that the suggested system accomplishes steady DC bus voltage, efficient power sharing between the battery and supercapacitor, and efficient power management. Composite energy storage system integration greatly enhances dynamic responsiveness while decreasing stress on batteries. The technology is also well-suited for contemporary DC microgrid applications since it guarantees dependable operation under changing load and PV generation circumstances.

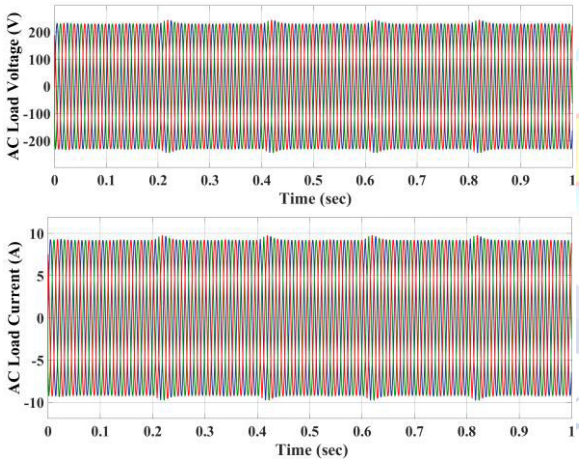

Fig.12 Simulation results of AC load voltage and current

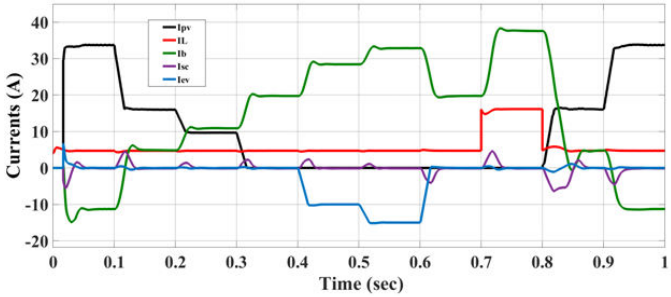

(a)

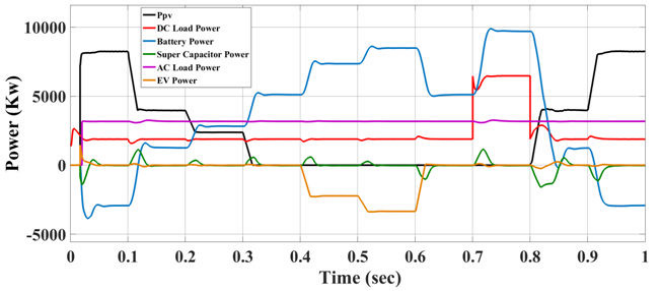

(b)

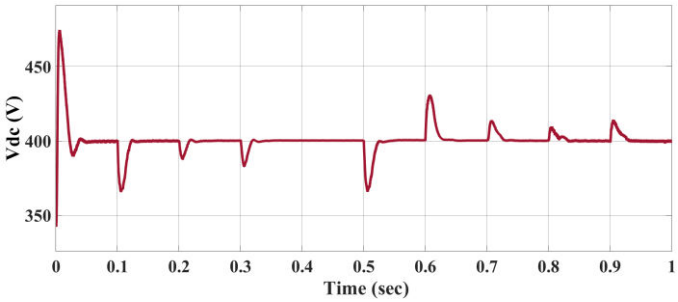

(C)

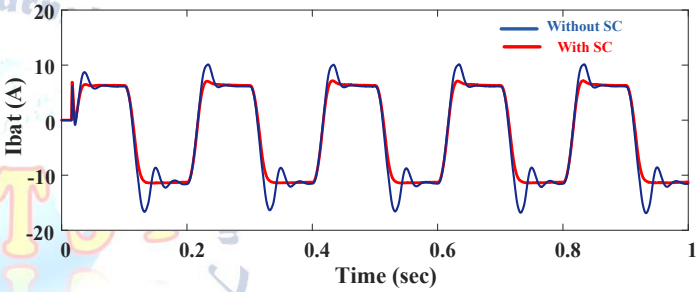

Fig. 13 Simulation results during power-sharing mode operation with the proposed DC microgrid (a) Current (b) Power (c) DC Link Voltage (d) Battery current without SC and with SC

CONCLUSION

This work presented the design and performance analysis of a multi-source DC-link integrated energy system consisting of a solar PV source, battery storage, supercapacitor, and EV charging load. The integration of all components through a common DC bus enables efficient power sharing and coordinated energy management under varying operating conditions. The use of a boost converter with MPPT ensures optimal utilization of solar energy, while bidirectional converters allow effective control of battery and supercapacitor charging and discharging. The results demonstrate that the supercapacitor effectively handles transient power fluctuations, reducing stress on the battery and improving its lifespan. The battery provides reliable energy support during low PV generation, ensuring

system continuity. The three-phase inverter enables stable AC load supply with improved power quality, while the EV charging unit operates efficiently through a controlled DC–DC converter. Overall, the proposed system shows improved dynamic response, enhanced stability, and efficient utilization of renewable energy. It offers a reliable and flexible solution for hybrid energy and EV applications. Future work can focus on advanced control strategies and real-time implementation to further enhance system performance.

Conflict of interest statement

Authors declare that they do not have any conflict of interest.

REFERENCES

[1] IEA, "Global EV Outlook 2023," International Energy Agency, 2023.

[2] M. Yilmaz and P. T. Krein, "Review of battery charger topologies for plug-in electric vehicles," IEEE Trans. Power Electron., vol. 28, no. 5, pp. 2151–2169, May 2013.

[3] B. Kroposki et al., "Achieving a 100% renewable grid," IEEE Power Energy Mag., vol. 15, no. 2, pp. 61–73, 2017.

[4] H. Lund et al., "Smart energy systems for sustainable energy," Energy, vol. 137, pp. 556–565, 2017.

[5] M. Rezkalla et al., "PV–wind hybrid renewable energy system for standalone applications," Energies, vol. 11, no. 10, p. 2790, 2018.

[6] A. Ghosh et al., "Sustainable hybrid renewable energy systems using optimization," Sustainable Energy Grids and Networks, vol. 21, 2020.

[7] N. Mohan, Power Electronics: Converters, Applications, and Design, Wiley, 2012.

[8] A. Y. Saber and G. K. Venayagamoorthy, "Plug-in vehicles and renewable energy sources," IEEE Trans. Ind. Electron., vol. 58, no. 4, pp. 1229–1238, 2011.

[9] T. Esram and P. L. Chapman, "Comparison of MPPT techniques," IEEE Trans. Energy Convers., vol. 22, no. 2, pp. 439–449, Jun. 2007.

[10] J. Ahmed and Z. Salam, "An improved P&O MPPT algorithm," IEEE Trans. Sustain. Energy, vol. 6, no. 3, pp. 909–919, 2015.

[11] S. Teleke et al., "Battery energy storage for wind farm dispatching," IEEE Trans. Energy Convers., vol. 24, no. 3, pp. 725–732, Sep. 2009.

[12] J. Cao and A. Emadi, "Battery/supercapacitor hybrid for EVs," IEEE Trans. Power Electron., vol. 27, no. 1, pp. 122–132, Jan. 2012.

[13] L. Zhang et al., "Hybrid energy storage management," IEEE Trans. Ind. Appl., vol. 53, no. 3, pp. 2567–2575, 2017.

[14] S. Jain et al., "Power management for hybrid battery-supercapacitor EVs," IEEE Trans. Ind. Electron., vol. 60, no. 12, pp. 5394–5402, 2013.

[15] Z. Song et al., "Energy management strategies review for hybrid EVs," Renew. Sustain. Energy Rev., vol. 40, pp. 365–383, Dec. 2014.

[16] H. Mahmood et al., "Power management in islanded PV-battery systems," IEEE J. Emerg. Sel. Topics Power Electron., vol. 2, no. 4, pp. 870–882, 2014.

[17] M. B. Camara et al., "Supercapacitor storage control for hybrid renewable systems," IEEE Trans. Ind. Electron., vol. 57, no. 12, pp. 4027–4035, 2010.

[18] Y. Jiang and X. Yu, "Microgrid energy management systems," Energies, vol. 12, no. 6, p. 1063, 2019.

[19] A. Khaligh and S. Dusmez, "Comprehensive review of EV charging," IEEE Trans. Ind. Electron., vol. 60, no. 8, pp. 3608–3619, Aug. 2013.

[20] H. Wang et al., "AC–DC power conversion system for EV charging," Energies, vol. 13, no. 14, p. 3690, 2020.

[21] M. Islam et al., "Simulation of hybrid EV charging station," Sustainable Cities and Society, vol. 62, 2020.

[22] D. Das et al., "Efficient bi-directional converter for EVs," IEEE Trans. Ind. Electron., vol. 65, no. 9, pp. 7271–7280, Sep. 2018.

[23] J. Wang et al., "Smart grid technologies for EVs," IEEE Trans. Ind. Appl., vol. 56, no. 3, pp. 2623–2635, 2020.

[24] N. Bizon, "Fuzzy energy management for smart grids with EVs," Energies, vol. 12, no. 4, p. 630, 2019.

[25] L. LIU ET AL., "ADVANCED HESS CONTROL IN MICROGRIDS," IEEE ACCESS, VOL. 9, PP. 115928–115947, 2021.